Field Crops Research 213 (2017) 12–20

Contents lists available at ScienceDirect

Field Crops Research

journal homepage: www.elsevier.com/locate/fcr

Improving fungal disease forecasts in winter wheat: A critical role of intra-day variations of meteorological conditions in the development of Septoria leaf blotch

Moussa El Jarroudi[a], Louis Kouadio[b], Mustapha El Jarroudi[c], Jürgen Junk[d], Clive Bock[e], Abdoul Aziz Diouf[a], Philippe Delfosse[d,*]

[a] Department of Environmental Sciences and Management, University of Liege, Arlon Campus Environnement, 185 Avenue de Longwy, Arlon, 6700, Belgium
[b] International Centre for Applied Climate Sciences, University of Southern Queensland, West Street, Toowoomba, QLD, 4350, Australia
[c] Laboratory of Mathematics and Applications, Department of Mathematics, Université Abdelmalek Essaâdi, B.P. 416, Tangier, Morocco
[d] Luxembourg Institute of Science and Technology, 41 Rue du Brill, L-4422 Belvaux, Luxembourg
[e] USDA-ARS-SEFTNRL, 21 Dunbar Road, Byron, GA 31008, United States

A R T I C L E I N F O

Keywords:
Temporal variability
Fourier transform method
Disease monitoring
Septoria leaf blotch
Weather

A B S T R A C T

Meteorological conditions are important factors in the development of fungal diseases in winter wheat and are the main inputs of the decision support systems used to forecast disease and thus determine timing for efficacious fungicide application. This study uses the Fourier transform method (FTM) to characterize temporal patterns of meteorological conditions between two neighbouring experimental sites used in a regional fungal disease monitoring and forecasting experiment in Luxembourg. Three meteorological variables (air temperature, relative humidity, and precipitation) were included, all conducive to infection of wheat by *Zymoseptoria tritici* cause of Septoria leaf blotch (STB) in winter wheat, from 2006 to 2009. The intraday, diurnal, dekadal and intra-seasonal variations of the meteorological variables were assessed using FTM, and the impact of existing contrasts between sites on the development of STB was analyzed. Although STB severities varied between sites and years ($P \leq 0.0003$), the results indicated that the two sites presented the same patterns of meteorological conditions when compared at larger temporal scales (diurnal to intra-seasonal scales, with time periods > 11 h). However, the intraday variations of all the variables were well discriminated between the sites and were highly correlated to STB severities. Our findings highlight and confirm the importance of intraday meteorological variation in the development of STB in winter wheat fields. Furthermore, the FTM approach has potential for identifying microclimatic conditions prevailing at given sites and could help in improving the prediction of disease forecast models used in regional warning systems.

1. Introduction

Integrated disease management based on decision support systems and disease forecasting models has become important more recently due to the increased need for sustainable practices in agriculture (Moreau and Maraite, 2000; Verreet et al., 2000; Audsley et al., 2005; Langvad and Noe, 2006). Reliable and timely information on plant fungal diseases epidemics are crucial for optimizing the use of fungicides while ensuring economic benefits (Fones and Gurr, 2015).

Plant disease epidemics of fungal origin result from the interaction between the pathogens, presence of susceptible hosts, and favourable meteorological conditions. Meteorological variables are most often the data used as inputs of disease forecasting models for fungal diseases of winter wheat (*Triticum aestivum* L.). Among the meteorological conditions, air temperature (T), relative humidity (RH), and precipitation (namely rainfall, R), are by far the most important. Numerous studies (e.g., Shaw and Royle, 1993; Eyal, 1999; Gladders et al., 2001; Lovell et al., 2004) have highlighted the effects of T, RH, and R on infection and progress of Septoria leaf blotch (STB, caused by *Zymoseptoria tritici* (Desm.) Quaedvlieg & Crous) in winter wheat. For the development of STB, T determines the rate at which fungal development and spore dispersal processes occur (Eyal, 1999; Gladders et al., 2001). A prolonged period of T below −2 °C has adverse effects on the fungus resulting in low survival and thus reduces inoculum to infect the wheat crop (Shaw and Royle, 1993). This, in turn, leads to a late or very slow development of the epidemic in the following spring even if weather

* Corresponding author.
E-mail address: philippe.delfosse@list.lu (P. Delfosse).

http://dx.doi.org/10.1016/j.fcr.2017.07.012
Received 2 May 2017; Received in revised form 17 July 2017; Accepted 19 July 2017

conditions are favourable (Lovell et al., 2004; El Jarroudi et al., 2009; Beyer et al., 2012). RH can affect the rate of plant disease epidemic development because micro-organisms generally grow (spore germination and infection) only when there is sufficient moisture (RH ≥ 60%) (Moreau and Maraite, 1999; El Jarroudi et al., 2009; Suffert et al., 2011). Rainfall is a key requirement for the development of STB as it allows for the swelling of pycnidia and aids the dispersal of spores in splash to the upper leaves of wheat plant (Shaw and Royle, 1993; Lovell et al., 1997; Gladders et al., 2001).

For disease risk assessments at the regional scale, the meteorological data used as main inputs for forecasting models originate from meteorological networks with automatic weather stations (AWS) (Gladders et al., 2001; Magarey et al., 2001; El Jarroudi et al., 2009; Te Beest et al., 2009; Beyer et al., 2012; Junk et al., 2016). Most often, these forecast models are based solely on the meteorological data from the nearest AWS or interpolated from a set of neighbouring sites. Interpolation procedures such as the nearest neighbour method, kriging, co-kriging, or inverse weighted-distance method are typically performed (Lam, 1983; Hartkamp et al., 1999; DeGaetano and Belcher, 2007). Although these schemes are used widely, they do suffer from some potential sources of error, e.g. difficulty in capturing small scale variation, failure to account for topographical features, etc. Furthermore, the choice of location for an AWS within a field or the distance between AWS locations are both factors that hamper accurate forecasting of fungal diseases at regional scales (Jones et al., 2012). Thus, to develop reliable disease forecasting models that can be applied efficiently in operational disease monitoring (i.e. embedded in a decision support system and applied at sub-regional and regional scales), a detailed analysis of weather data, both spatially and temporally, is of great importance (Henshall et al., 2016; Donatelli et al., 2017). Indeed, the difference in weather conditions between neighbouring wheat fields (5–15 km, straight line) is often not perceptible, yet crucial in disease forecast models.

Fourier transform methods (FTMs) constitute one of the most widely used operations to obtain a spectral representation of a time series of discrete data samples (Chatfield, 1996; Blommfield, 2000; Brillinger, 2002; Craigmile and Guttorp, 2011; Mikosch and Zhao, 2014). Although they have been used for several and various purposes (e.g. Estrada-Pena et al., 2014; Mikosch and Zhao, 2014), their application for weather data analysis and plant disease development has yet to be fully investigated. In this study we investigate the causes of difference in STB expression across neighbouring locations based on the analysis of weather patterns at various temporal scales. First, a comprehensive theoretical framework of linear spectral analyses based on FTM, along with a conceptual framework, was devised. Then the approach was applied to a case study of two neighbouring sites included in a regional fungal disease monitoring and forecasting experiment.

2. Materials and methods

2.1. Theoretical framework of the Fourier transform method

FTM principles have been discussed extensively (e.g., Jones, 1964; Bergland, 1969; Chatfield, 1996; Blommfield, 2000). Only some general principles were summarized in the following paragraphs.

A filtered series Y_t is a weighted sum of the time series (the discrete data samples) X_t defined as,

$$Y_t = \sum_{k=-\infty}^{+\infty} a_k X_{t-k},$$

where the basis numbers a_k verify $\sum_{k=-\infty}^{+\infty} a_k = 1$. The sequence $a = (a_k)_{k\in Z}$ is called a linear filter. The Fourier transform of the filtered series, $F_Y(\lambda)$, is the product of the Fourier transform of the filter a and the Fourier transform of the original time series X_t, that is (Chatfield, 1996; Blommfield, 2000),

$$F_Y(\lambda) = F_a(\lambda)\cdot F_X(\lambda).$$

where λ is the frequency, and $F_a(\lambda)$ is the Fourier transform of the filter a given as,

$$F_a(\lambda) = \sum_{k=-\infty}^{+\infty} a_k e^{-i\lambda k}$$

and $F_X(\lambda)$ is the Fourier transform (or discrete-time Fourier transform) of the time series X_t given for a finite duration sequence of length n by

$$F_X(\lambda) = \sum_{t=0}^{n-1} X_t e^{-i\lambda t} \ ,$$

where $i = \sqrt{-1}$. For $\lambda = \frac{2\pi k}{n}$, k = 0, 1,…, n − 1, we obtain the discrete Fourier transform applied to the discrete-time series X_t through

$$\hat{X}(k) = F_X\left(\frac{2\pi k}{n}\right) = \sum_{t=0}^{n-1} X_t e^{-i\frac{2\pi kt}{n}},$$

with the corresponding inverse discrete Fourier transform

$$X_t = \frac{1}{n}\sum_{k=0}^{n-1} \hat{X}(k) e^{i\frac{2\pi kt}{n}},$$

where $\hat{X}(k)$ represents the frequency domain function and X_t the time domain function. Using this pair of formulae, we can move back and forth between a time representation of data $(X_t)_{t\ =\ 0\ ,...,\ n-1}$ and its frequency domain representation $(\hat{X})_{t\ =\ 0,\ ....\ ,\ n-1}$ that is, the discrete Fourier transform is invertible. Also, it is possible to modify the frequency spectrum in order to change the time representation, i.e. to allow the filtering.

The Fourier transform of the linear filter a (denoted B) is called the transfer function of the linear filter. The transfer function B describes how the amplitude (corresponding to the standard deviation) is transferred from X to Y, and the quantity $|B|^2$ describes how the energy (variance) is transferred from the original series X to the filtered series Y. For a simple moving average filter q defined through $a = (a_k)_{k\in Z}$, with

$$a_k = \begin{cases} \frac{1}{2q+1} & \text{if } k \in \{-q, ..., +q\}, \\ 0 & \text{otherwise}, \end{cases}$$

we have $B = \frac{1}{2q+1}\sum_{k=0}^{2q} e^{-ik\lambda} = \frac{1}{2q+1}\frac{1-e^{-i\lambda(2q+1)}}{1-e^{-i\lambda}}$ and $|B|^2 = \left(\frac{1}{2q+1}\right)^2 \frac{\sin^2\left(\frac{\lambda(2q+1)}{2}\right)}{\sin^2\left(\frac{\lambda}{2}\right)}$.

2.2. Conceptual approach of the FTM

The conceptual approach uses a mathematical function called *KZ* transformation (Zurbenko, 1986; Hogrefe et al., 2000) which is based on a linear filter q. This linear filter is a simple moving average iterated k times. The function *KZ* is identified as a function of the variables *X, q, k*, where *X* is a given meteorological variable, q is the linear filter associated to the moving average, and k refers to the iterations (in our study k varies between 1 and 3). *KZ* can be expressed in terms of the Fourier transform involving a series of equations with a sampling interval (or time frequency) 1/2 Δt (indeed the time scale is a minimum of 2 h, thus 1/2 Δt = 1 h). To find the power transfer function for the *KZ(q, k)*-function, the rule of sequential filtering is applied, that is,

$$|B|^2 = \left\{\left(\frac{1}{2q+1}\right)^2 \frac{\sin^2\left(\frac{\lambda(2q+1)}{2}\right)}{\sin^2\left(\frac{\lambda}{2}\right)}\right\}^k$$

Based on the *KZ*-function and the filter q, a given meteorological variable is decomposed in a series of filtered data. For each

Table 1
Agronomic information for winter wheat fields at the study sites in Luxembourg during the 2006–2009 cropping seasons.

Site	Year	Cultivar	STB susceptibility[a]	Sowing date	Harvest date	Previous crop
Christnach	2006	Flair	4	12 Oct. 2005	25 Jul. 2006	Maize
	2007	Tommi	4	12 Oct. 2006	26 Jul. 2007	Maize
	2008	Flair	4	23 Oct. 2007	5 Aug. 2008	Maize
	2009	Boomer	5	23 Oct. 2008	6 Aug. 2009	Maize
Everlange	2006	Flair	4	10 Oct. 2005	7 Aug. 2006	Fallow
	2007	Flair	4	10 Oct. 2006	26 Jul. 2007	Pea
	2008	Tommi	4	8 Oct. 2007	5 Aug. 2008	Fallow
	2009	Achat	5	13 Oct. 2008	6 Aug. 2009	Oilseed rape

[a] SLB susceptibility: Scale 1 (low susceptibility) to 9 (high susceptibility) (BSA 2008).

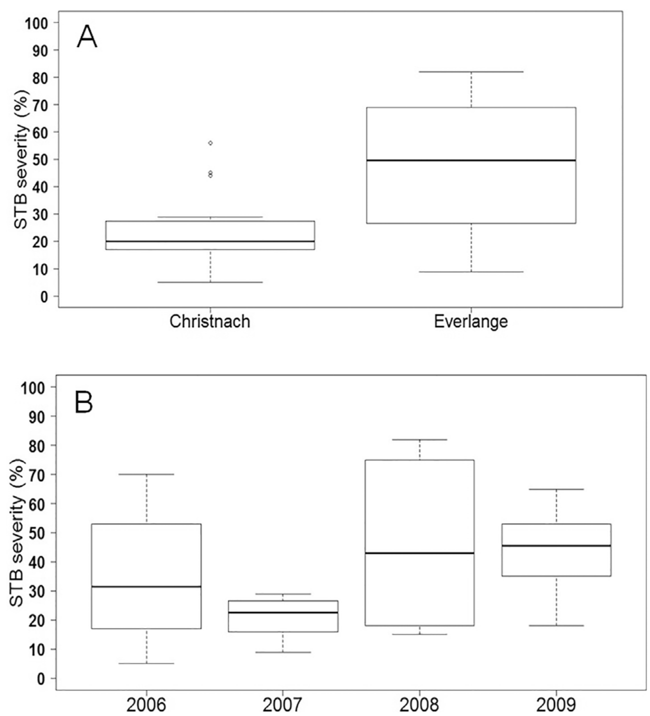

Fig. 1. Boxplot of the average Septoria leaf blotch (STB) severity during GS 75 to GS 85/87 by site (A) and year (B). Data from control plots were used (n = 4 per site and per year).

meteorological variable, we have:

$$Y_t = \frac{1}{2q+1}\sum_{i=-q}^{q} X_{t-i}\ ,$$

$$Z_t = \frac{1}{2q+1}\sum_{i=-q}^{q} Y_{t-i}\ ,$$

$$W_t = \frac{1}{2q+1}\sum_{i=-q}^{q} Z_{t-i}\ ,$$

Where t = time (hours); i = the index; q = the filter; X_t = the actual value at time t, and Y_t = the predicted value at time t; Z_t is the iteration of the predicted value Y_t at time t (i.e. its Fourier transform) and W_t is the Fourier transform of the iteration Z_t. The same moving average filter q is applied here 3 times sequentially (k = 3) giving,

$$F_Y(\lambda) = \left(\frac{1}{2q+1}\frac{1-e^{-i\lambda(2q+1)}}{1-e^{-i\lambda}}\right)\cdot F_X(\lambda),$$

$$F_Z(\lambda) = \left(\frac{1}{2q+1}\frac{1-e^{-i\lambda(2q+1)}}{1-e^{-i\lambda}}\right)^2\cdot F_X(\lambda),$$

$$F_W(\lambda) = \left(\frac{1}{2q+1}\frac{1-e^{-i\lambda(2q+1)}}{1-e^{-i\lambda}}\right)^3\cdot F_X(\lambda).$$

The different meteorological variables considered for our study are T, RH and R. Thus, the previous equations can be summarized as follows for T, RH, and R:

$$T_{13} = KZ(T,\ q=1,\ k=3);\ RH_{13} = KZ(RH,\ q=1,\ k=3);\ R_{13} = KZ(R,\ q=1,\ k=3);$$

$$T_{63} = KZ(T,\ q=6,\ k=3);\ RH_{63} = KZ(RH,\ q=6,\ k=3);\ R_{63} = KZ(R,\ q=6,\ k=3);$$

$$T_{120} = KZ(T,\ q=120,\ k=3);\ RH_{120} = KZ(RH,\ q=120,\ k=3);\ R_{120} = KZ(R,\ q=120,\ k=3)$$

Depending on the value of the linear filter, the amplitude of the analysed parameter can be viewed within day (intraday), between days (diurnal), within a dekade (dekadal) or within the season (intra-seasonal). The value of the filter is low (i.e. q = 1) for small changes and increases gradually as the variation becomes important. The choice of temporal windows was based on Horne and Baliunas (1986) and Gilliam et al. (2006).

Thus, we define the intraday variation, W_{ID}, as the tendency of each meteorological variable in the day (< 11 h) from a moving average filter q = 1, given by,

$W_{ID} = X_t - W_t(q = 1)$.

The intraday variation for T, RH, and R is calculated as: $T_{ID} = T - T_{13}$, $RH_{ID} = RH - RH_{13}$, and $R_{ID} = R - R_{13}$, respectively.

The diurnal variation, W_{DU}, refers to the tendency of each meteorological variable between 11 and 48 h which follows in general the set of intraday variations. It is given by,

$W_{DU} = W_t\ (q = 1) - W_t(q = 6)$; that is, for T, RH, and R, $T_{DU} = T_{24} = T_{13} - T_{63}$, $RH_{24} = RH_{13} - RH_{63}$, and $R_{24} = R_{13} - R_{63}$, respectively.

The dekadal variation, W_{DK}, is the tendency of each meteorological variable between 48 h to 40 days. W_{DK} is given by,

$W_{DK} = W_t\ (q = 6) - W_t\ (q = 120)$; that is, for T, RH, and R, $T_{DK} = T_{63} - T_{120}$, $RH_{DK} = RH_{63} - RH_{120}$, and $R_{DK} = R_{63} - R_{120}$, respectively.

The intra-seasonal variation, W_{IS}, represents the tendency over a long period (> 40 days) and it given by (moving average with filter q = 120),

$W_{IS} = W_t(q = 120)$; that is, for T, RH, and R, $T_{IS} = T_{120}$, $RH_{IS} = RH_{120}$, and $R_{IS} = R_{120}$, respectively.

2.3. Study sites, disease infection simulation, field experiments and disease severity assessment

To characterize the patterns of T, RH and R, the FTM was performed using data from two sites, one located at Christnach (49°47′N, 6°16′E,

Table 2
Timing of the development of wheat plants (growth stages) at Christnach and Everlange in Luxembourg during the 2006–2009 cropping seasons.

Site	Year	GS45[a]	GS59	GS69	GS75	GS85
Christnach	2006	29 May	12 June	19 June	26 June	n.a.[b]
	2007	14 May	21 May	29 May	11 June	18 June
	2008	26 May	02 June	09 June	30 June	07 July
	2009	25 May	02 June	15 June	22 June	29 June
Everlange	2006	29 May	06 June	12 June	26 June	n.a.
	2007	14 May	21 May	29 May	11 June	18 June
	2008	26 May	02 June	09 June	30 June	07 July
	2009	25 May	02 June	15 June	22 June	29 June

[a] GS: Zadoks' growth stage (Zadoks et al., 1974).
[b] Not applicable.

elevation 313 m) and the second at Everlange (49°46′N, 5°57′E, elevation 309 m). Both sites are located in the Gutland region which is a region of lower elevation consisting of hills and broad valleys (Luxembourg has two topographic regions; the second being the Oesling region). The distance (straight line) between the sites is approximately 15 km. Hourly meteorological data covering the 2006–2009 growing seasons for winter wheat were used (Table 1). They were retrieved from a web-based database (www.agrimeteo.lu) and processed using an automatic data processing chain for quality check and gap filling (Junk et al., 2008).

STB incidence and severity were monitored during the 2006–2009 cropping seasons. Wheat varieties with the same susceptibility to STB were grown at the two sites (Table 1). The trials were designed in a randomized block with four replicates (one replicate plot = 12 m^2). Each replicate block consisted of fungicide treated and non-treated (control) plots, but only assessments from control plots were used in this study. The assessments of STB severity were made weekly from growth stage (GS) 29/30 to GS 85/87 (Zadoks et al., 1974) on the same 10 plants. Care was taken to minimize errors in disease estimates by training raters using standard area diagrams and disease assessment software and ensuring the same raters assessed the same experiments in each season (El Jarroudi et al., 2014).

Along with field observations, the STB development at the selected sites was also simulated using the disease forecast model PROCULTURE (Moreau and Maraite, 2000). The ability of the PROCULTURE model to reliably predict STB occurrences at the two sites has been successfully demonstrated (see El Jarroudi et al., 2009). In PROCULTURE, specific meteorological conditions must be met for infection to occur: during a 2-h rainfall event, the rainfall in the first hour must be at least 0.1 mm, followed by a second hour of rainfall with at least 0.5 mm. In addition to the rainfall, RH must be higher than 60% during the 16 h following the rain event, and T must remain above 4 °C for 24 h (Moreau and Maraite, 1999; El Jarroudi et al., 2009).

2.4. Data analysis

Observed meteorological data from the 1 May–30 June period were filtered based on the conceptual FTM approach defined previously. The 1 May–30 June period includes the critical period for STB infections in wheat at the two study sites, i.e. the period spanning the development of the three upper leaves L1-L3 (L1 being the flag leaf) when STB infections are most likely to result in yield reduction (El Jarroudi et al., 2012; El Jarroudi et al., 2015). Indeed, these upper leaves are the main contributors to grain filling, and therefore to grain yield, in wheat. STB development conditions on these leaves were compared over the same period. We assumed that spores of *Z. tritici* are present in sufficient numbers to infect leaves at both sites and that any difference in STB development was due solely to the meteorological conditions. Contrasts between sites at the different temporal scales (i.e., intraday, diurnal, dekadal and intra-seasonal, as defined above) were assessed through

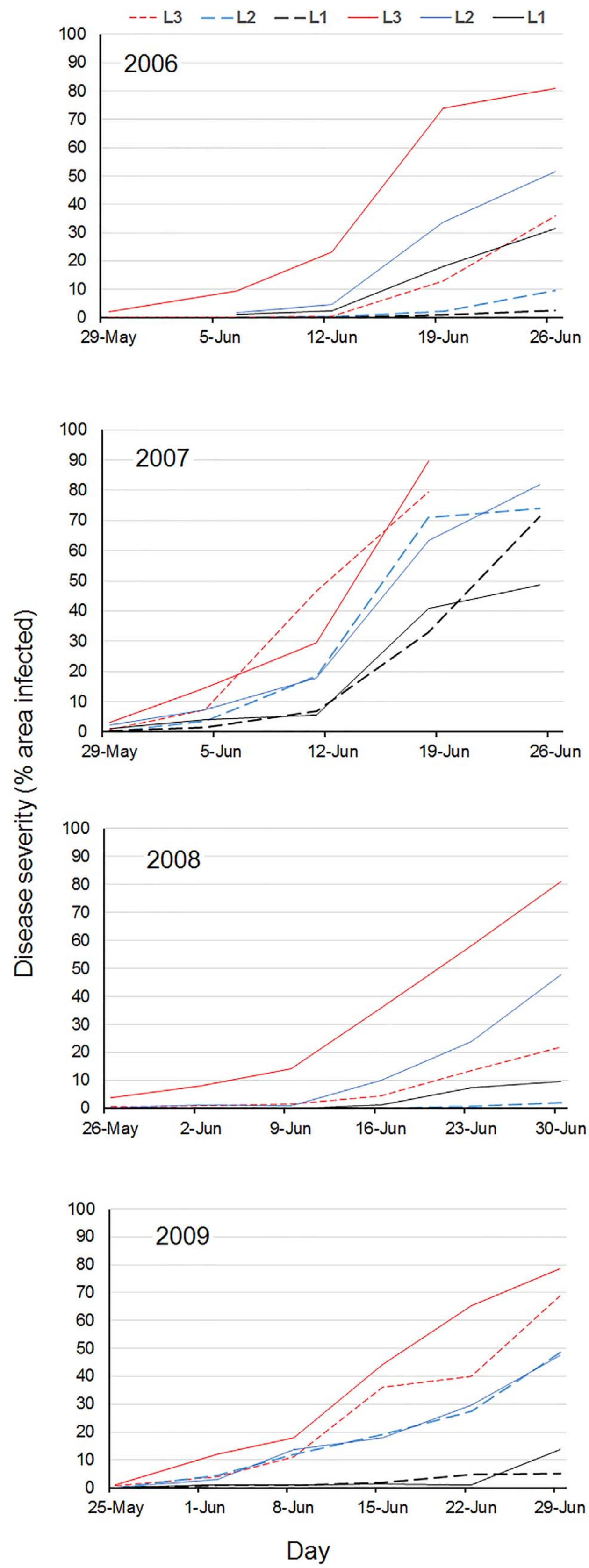

Fig. 2. Septoria leaf blotch (STB) severity on the three upper leaves L1-L3 (L1 being the flag leaf) from the last week of May to the end of June at Christnach (dashed lines) and Everlange (solid lines) during the 2006–2009 cropping seasons. The start period was determined by the first appearances of STB on L3. At both sites this occurred during the last 2 weeks of May during the study period. In 2008 at Christnach the maximum STB severity percentage on L1 was 0.2%.

Table 3
Pearson's product-moment correlation coefficients of selected meteorological variables between Everlange and Christnach over the 2006–2009 cropping seasons. The comparisons were performed using hourly raw data (before filtering) and filtered data (filtering using a Fourier transform method at different temporal scales) over the period 1 May–30 June. The intra-seasonal scale include an extended period (April–June).

Year	Variable	Before filtering	After filtering			
			Intraday scale (< 11 h)	Diurnal scale (11–48 h)	Dekadal scale (2–40 d)	Intra-seasonal scale (> > 40 d)
2006	Air temperature	0.949	0.453	0.968	0.973	0.999
	Relative humidity	0.881	0.370	0.915	0.910	0.981
	Rainfall	0.543	0.273	0.731	0.898	0.999
2007	Air temperature	0.954	0.537	0.959	0.979	0.994
	Relative humidity	0.781	0.008[a]	0.683	0.846	0.991
	Rainfall	0.502	0.299	0.663	0.740	0.335
2008	Air temperature	0.956	0.430	0.968	0.992	0.998
	Relative humidity	0.925	0.308	0.950	0.959	0.938
	Rainfall	0.165	−0.049[b]	0.445	0.515	−0.210
2009	Air temperature	0.976	0.553	0.983	0.987	0.982
	Relative humidity	0.726	0.418	0.971	0.968	0.998
	Rainfall	0.957	0.480	0.875	0.954	0.992

Note: $P < 0.0001$ in all cases except in [a] and [b] where $P = 0.7$ and 0.08, respectively.

correlation analyses using their non-filtered and filtered meteorological data. Additionally, the average STB severity on L1-L3 during GS 75 to GS 85/87 stages were compared between sites over the study period to determine whether there were any difference in disease severity. The progress of STB on the three upper leaves was assessed based on the variations of the meteorological variables at these different temporal scales. All analyses were performed in R (R Development Core Team, 2014) and MS Excel (Microsoft, Redmond, WA).

3. Results

3.1. Septoria leaf blotch severity at the study sites

The average severity of STB during GS 75 to GS 85/87 over the study period for the two sites is presented in Fig. 1. The two way ANOVA carried out on the average disease severity by site and year indicated a statistically significant difference between sites [$F(1,24) = 40.24$, $P < 0.0001$] and between years [$F(3,24) = 9.19$, $P = 0.0003$], as well as a significant interaction between the two effects [$F(3,24) = 15.31$, $P < 0.0001$]. Normality checks and Levene's test were carried out and the assumptions were met. Tukey's HSD post hoc tests were carried out. For the years 2006 and 2008, the average STB severity at Everlange was significantly different to that of Christnach ($P = 0.0008$ and < 0.0001, respectively). For 2007 and 2009 no statistical difference was found.

The temporal development of the wheat plant is indicated by the dates at which each growth stage was attained (Table 2). There was a range in STB severity among sites and years during the critical period for STB development on L1-L3 (Fig. 2). Overall, there was a trend for an increase in STB on L1-L3 throughout the season each year, with marked differences between sites for the same leaf in all years, except in 2007. The differences were particularly striking during June. For example, on 19 June 2006, the severity of STB was 13% on L3 at Christnach, while it was 74% at Everlange (Fig. 2). In 2007 and 2009, the difference in STB severity on all leaves was less pronounced (< 10%), except on L3 in 2009. It should be noted that other foliar diseases including wheat leaf rust and powdery mildew were observed at the selected sites during the study period (El Jarroudi et al., 2012). Indeed, during GS 77 and GS 87 the average severity of wheat leaf rust on the three upper leaves over the 4-year period ranged from 4 to 15% at Everlange (with most severe rust in 2008 and 2009) and 1–22% at Christnach (with most severe rust in 2007). The average severity of powdery mildew was less than 5% at both sites during the same period.

3.2. Temporal patterns of air temperature, relative humidity and rainfall

The FTM approach was used to distinguish the patterns of meteorological conditions between the two sites over the study period. Non-filtered data for T and RH were highly correlated ($r \geq 0.726$, $P < 0.0001$; Table 3). However, non-filtered data for R showed a range in correlation ($r = 0.165$ to 0.957, $P < 0.0001$) between sites over the 4-year study period. With filters applied, the intraday variation for T, RH and R were contrasted between the two sites. The correlations (r) ranged from 0.430 to 0.553 ($P < 0.0001$), 0.008 ($P = 0.7632$) to 0.418 ($P < 0.0001$), and −0.049 ($P = 0.0819$) to 0.480 ($P < 0.0001$), for T, RH and R respectively (Table 3). At the diurnal to intra-seasonal scales association among meteorological variables between the two sites remained strong for both T and RH ($r \geq 0.683$, $P < 0.0001$; Table 3). However for R, weak associations between the two sites were observed at the intra-seasonal scale in 2007 and 2008 ($r = 0.335$ and −0.210, respectively; $P < 0.0001$ for both correlations), and strong associations were mostly found for diurnal to intra-seasonal scales in 2006 and 2009 (Table 3). A graphical trend analysis of the meteorological variables was performed. An example of the variations at the different temporal scales over the period May-June 2006 is shown in Fig. 3A–L. The trends presented here for 2006 did not differ greatly from the same period in the remaining years (Supplementary Figs. S1–S3). The trend and amplitude in T in 2006 were pronounced at the intraday (Fig. 3A) and diurnal scales (Fig. 3D), with values at Everlange higher in most cases (particularly at the intraday scale). There was a clear difference in patterns of RH between sites at the intraday scale (Fig. 3B). Overall, the trends at the diurnal and dekadal scales were similar (Fig. 3E and H), although there were some discernible differences in amplitude at the intra-seasonal scales (Fig. 3K). Noticeable differences in trend and amplitude in R at all temporal scales were found between Christnach and Everlange (Fig. 3C, F, I and L). The amplitudes recorded for R over larger temporal scales (dekadal to intra-seasonal) might be explained by the time required for rain-bearing cloud to move from one site to the other, or by localised, small-scale convective events (summer storms). Overall, these findings provide insight into the contrast in meteorological patterns at different scales between the two sites, which are only 15 km apart; for each of the meteorological variables this was noticeable at small temporal scales, namely at the intraday scale.

3.3. Relationships between STB development and the meteorological patterns

The number of infection days predicted by PROCULTURE during the

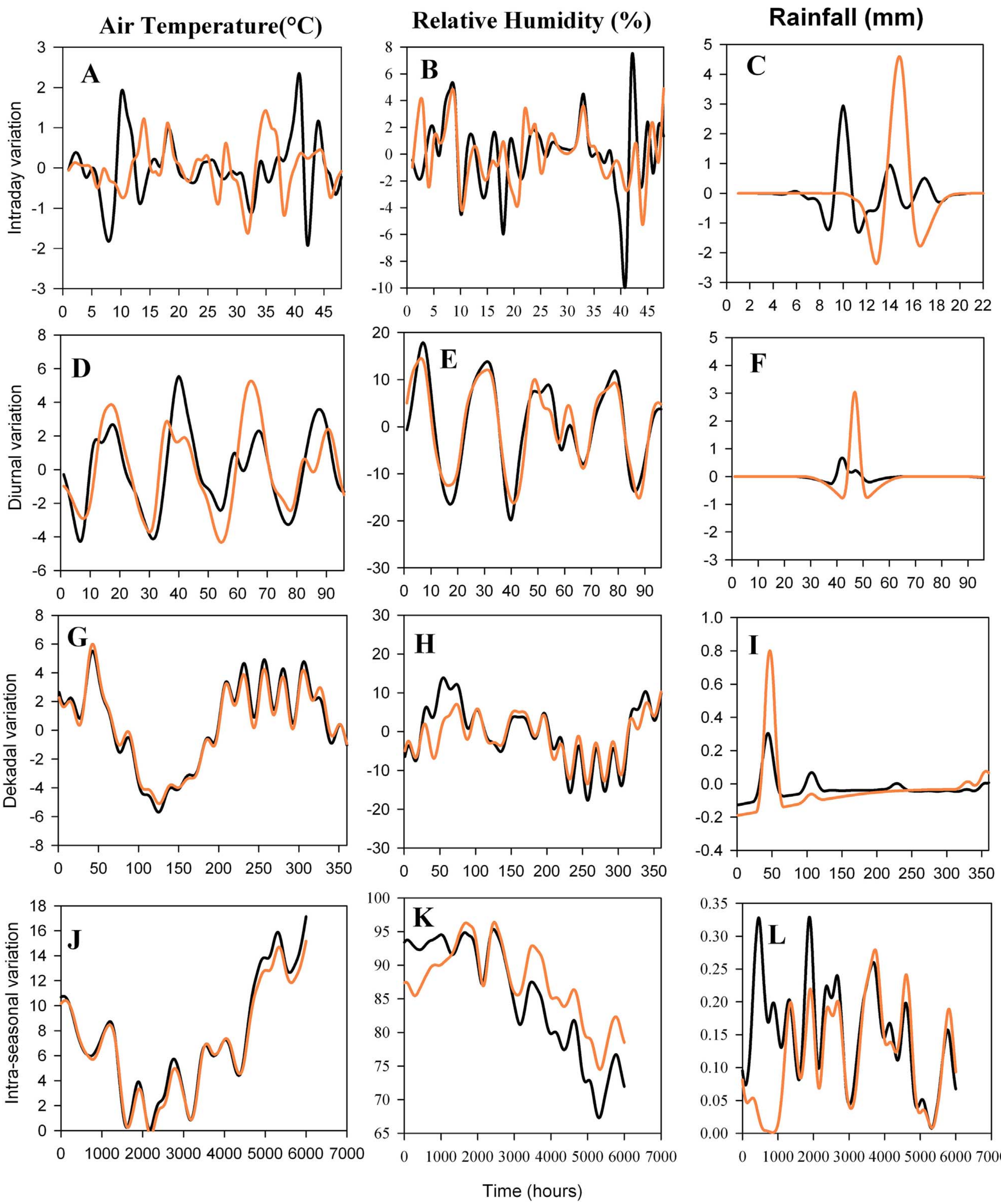

Fig. 3. Example of the variations in air temperature (*T*), relative humidity (*RH*) and rainfall (*R*) at different temporal scales at Christnach (orange lines) and Everlange black lines). **A–C**: intraday variation of *T*, *RH* and *R*, respectively. **D–F**: diurnal variation of *T*, *RH* and *R*, respectively. **G–I**: dekadal variation of *T*, *RH* and *R*, respectively. **J–L**: dekadal variation of *T*, *RH* and *R*, respectively. The intraday, diurnal and dekadal scales are computed over the period 1 May–30 June 2006. Whereas the intra-seasonal scale is computed over the period October 2005–June 2006. (For interpretation of the references to colour in this figure legend, the reader is referred to the web version of this article.)

period critical for infection with *Z. tritici* indicates that there was a relatively high number of days at Everlange in 2006, 2007 and 2009 (Table 4), although the STB severity observed at Everlange was higher compared to that at Christnach in all years, except 2007 (Fig. 2). For the period May-June 2006, a detailed analysis of *Z. tritici* favourable infection periods and intraday variations in meteorological variables indicates that on 15 June 2006 *Z. tritici* favourable infection periods were recorded at Everlange but not at Christnach (Fig. 4). The amplitudes in T and RH at the intraday scale were very pronounced at Everlange, while at Christnach only variations in temperature were pronounced. Thus, while the comparison based on non-filtered data resulted in similar meteorological pattern between sites (and would

Table 4
The number of infection days for *Zymoseptoria tritici* (cause of Septoria leaf blotch) as simulated by the PROCULTURE model between 1 May and 30 June at Christnach and Everlange during the 2006–2009 cropping season.

Year	Christnach	Everlange
2006	9	16
2007	16	23
2008	11	12
2009	14	16

have not explained the differences relating to infection conditions), the combined effects of intraday variation of T and RH provide valuable information and a better basis for understanding differences between sites. Similar differences in conditions were observed in the different cropping seasons (for example, in years 2007 and 2008, Supplementary Figs. S4 and S5, respectively).

Furthermore, an analysis of PROCULTURE outputs shows a difference between the two sites and the existence of an offset for the infection periods. An example is given in Fig. 5 for illustration purpose. In this case, at Everlange L5 was infected on 1 April, whereas L4 and L3 were infected on 1 May, and L2 and L1 on 7 June. However, at Christnach, although L5-L3 were infected during the same period as at Everlange, L2 and L1 were infected almost one week earlier (end of May).

For instance, if the meteorological conditions T = 4 °C, RH = 90%, and R = 0.1 mm were recorded at 2 p.m. at Everlange, and T = 3 °C, RH = 92%, and R = 0 mm were recorded at the same time at Christnach, PROCULTURE would indicate the start of an infection period only at Everlange (with subsequent STB development being more severe at this site); whilst the comparison of meteorological conditions would give a good correlation between the two sites and thus suggest similar development of STB. In such cases the spectral decomposition analysis of T, RH and R would reveal the difference between sites at the intraday scale rather than at the diurnal scale over the period considered, thereby providing the insight needed to differentiate disease development at the two sites.

4. Discussion

Developing an adequate disease forecasting model requires detailed analysis of available weather data in relation to disease development. The density of the weather stations in the field, as well as the applicable area represented by each of the weather stations are critical features in determining the accuracy of the interpolated values for each variable. Given the potential adverse impacts of fungal diseases and the environmental concerns of fungicides, sophisticated forecasting models are needed to minimise and improve the timing of control measures (Te Beest et al., 2009; Lucas, 2011; Shtienberg, 2013; Small et al., 2015). In operational warning systems for plant diseases at regional scale, a close examination of stations that exhibit quite similar patterns of weather conditions, but have crops with contrasting disease development despite cultivars with the same susceptibility, deserves special attention as a basis for the improvement of the forecasting systems.

We investigated the application of the Fourier transform method for frequency domain analysis of three meteorological variables (T, RH and R) between two relatively close sites which are part of the framework of an operational warning system for fungal diseases of winter wheat in Luxembourg (El Jarroudi et al., 2015). Findings indicate that there was a contrast in intraday variations between the two sites for all the meteorological variables. But when compared at diurnal, dekadal and intra-seasonal scales, the sites behaved quite similarly. The difference between sites at the intraday temporal scale can be explained, partly, by the type of rain, its persistence and its distribution in space and time, especially during the stem elongation phase of winter wheat (GS 30 to GS 39) where convective events (e.g. summer storms) are frequent in Luxembourg. Mahtour et al. (2011) noted that radar technology provided better estimates of rainfall occurrence over a continuous space than AWS, but deriving absolute precipitation values from radar data is still challenging. The topography, direction of prevailing winds or distance from large bodies of water, not evaluated in detail in this study, may also explain the amplitude fluctuations of the meteorological variables studied between the sites (Kuuseoks et al., 1997; Magarey et al., 2001).

The analysis of the variations of meteorological conditions at different temporal scales and STB progress on the three upper leaves in winter wheat was based on the assumption that at both sites spore availability and dispersal were the same in a given year. Fungal disease epidemic progress from small to larger scales may vary greatly within and between sites. The impact of *Z. tritici* spore dispersal at the study sites was not investigated here. Although modelling spore dispersal at different spatial scales remains challenging (namely because of the complexity of inoculum dispersal processes, the difficulty of collecting empirical dispersal data at relevant spatial scales, and the mathematical

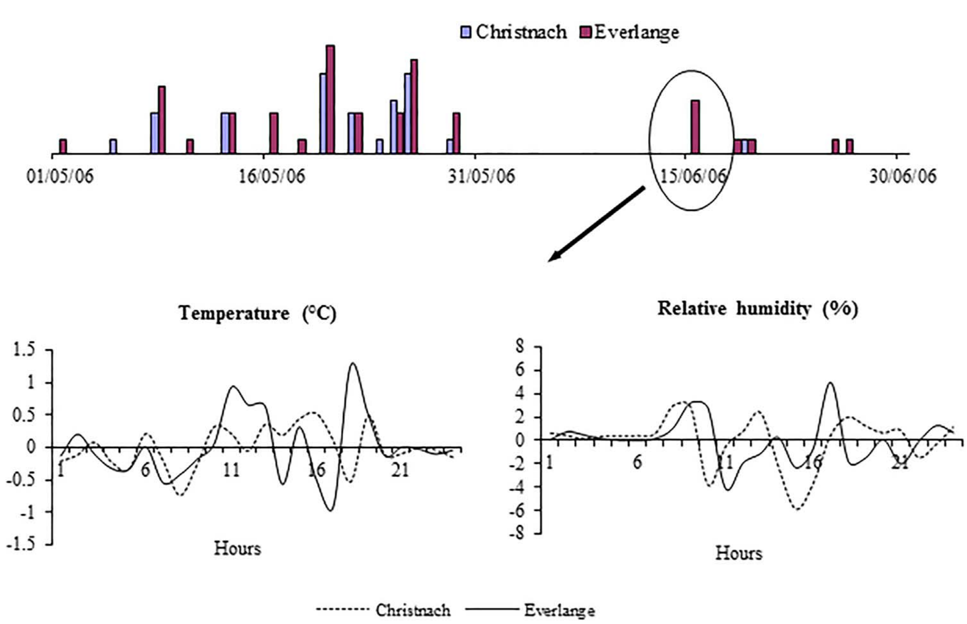

Fig. 4. The simulated number of infections periods for *Zymoseptoria tritici* (cause of Septoria leaf blotch) during the period 1 May–30 June 2006 at Christnach and Everlange. An example of the variations in temperature and relative humidity at the intra-day scale for the 15 June is shown in order to demonstrate the difference between sites.

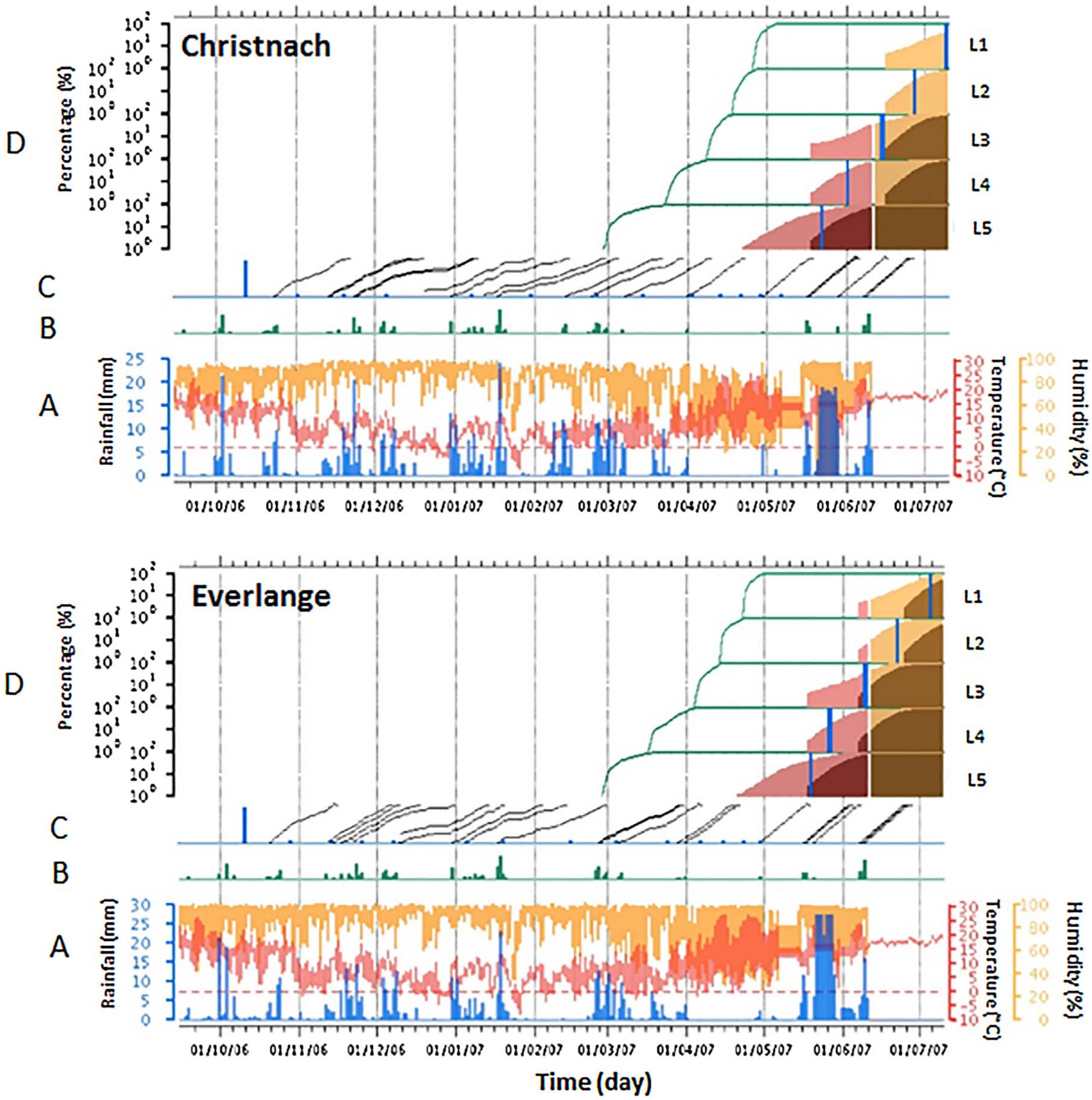

Fig. 5. Outputs of the PROCULTURE model for Christnach (upper chart) and Everlange (lower chart) sites, 2006–2007 cropping season. **A:** Average daily air temperature (°C, red lines), relative humidity (%, orange lines), and rainfall (mm, blue bars) as recorded by the automatic weather stations. **B:** Number of hours per day with a high probability of infection by *Zymoseptoria tritici* (cause of Septoria leaf blotch, STB). **C:** Latency periods of STB (blue bars) and latency period durations (black lines). **D**: Percentage of leaf area development (green lines), observed start date of leaf senescence (blue bars), actual STB severity (%, primary infections pink areas, secondary infections dark pinAk areas) and simulated STB severity (primary infections light brown, and secondary ones dark brown areas) for leaves L5 to L1 (L1 being the flag leaf). (For interpretation of the references to colour in this figure legend, the reader is referred to the web version of this article.)

complexity of atmospheric dispersion models; Shaw, 1994a,b; Brown and Hovmøller, 2002; Filipe and Maule, 2004; Garrett et al., 2011), warning systems like those employed in Luxembourg for fungal disease monitoring would benefit from such integrated FTM approaches and spore dispersal modelling. This remains an area open for further research.

Fourier-transformed data/methods have been used in many epidemiological studies, including the description of plant pathogen population progress throughout cropping seasons (e.g. Shaw, 1994b), building outperforming data sets for characterizing the abiotic niches of parasitic organisms (e.g. Estrada-Pena et al., 2014), or as automation method for fungal spore detection (e.g. Hahn, 2002). In our case study STB was selected and studied in relation to filtered patterns of T, RH and R. A similar FTM approach can be used with other meteorological data and for other economically important fungal pathogens for explaining the spatial variations in disease. For reliable monitoring of fungal diseases at regional scales, the spatial distribution and representativeness of weather data is crucial. FTM might be a suitable approach to determine the minimum distance between fixed stations by analysing the intraday amplitudes of the primary meteorological variables. Determining this distance will enable informed decisions to be made regarding the number and positioning of weather stations, in turn allowing a better differentiation between sites and thereby ensuring an accurate, site-specific disease forecast model. The FTM approach has potential for specifying the microclimate conditions prevailing at given sites and could help improve the prediction accuracy of disease forecast models involved in regional warning systems and decision support systems.

Acknowledgments

The research was funded by the Ministry of Higher Education and Research of the Grand-Duchy of Luxembourg and the Administration des Services Techniques de l'Agriculture through the MACRY and

SENTINELLE projects.

Appendix A. Supplementary data

Supplementary data associated with this article can be found, in the online version, at http://dx.doi.org/10.1016/j.fcr.2017.07.012.

References

Audsley, E., Milne, A., Paveley, N., 2005. A foliar disease model for use in wheat disease management decision support systems. Ann. Appl. Biol. 147, 161–172.

Bergland, G.D., 1969. A guided tour of the fast Fourier transform. IEEE Spectr. 6, 41–52.

Beyer, M., El Jarroudi, M., Junk, J., Pogoda, F., Dubos, T., Görgen, K., Hoffmann, L., 2012. Spring air temperature accounts for the bimodal temporal distribution of Septoria tritici epidemics in the winter wheat stands of Luxembourg. Crop Prot. 42, 250–255.

Blommfield, P., 2000. Fourrier analysis of time series, an introduction, 2nd edition. Wiley and Sons, New York, USA.

Brillinger, D.R., 2002. John W. Tukey's work on time series and spectrum analysis. Ann. Stat. 1595–1618.

Brown, J.K.M., Hovmøller, M.S., 2002. Aerial dispersal of pathogens on the global and continental scales and its impact on plant disease. Science 297, 537–541.

Chatfield, C., 1996. The Analysis of Time Series: An Introduction, 5th edition. Chapman and Hall, London, UK.

Craigmile, P.F., Guttorp, P., 2011. Space-time modelling of trends in temperature series. J. Time Ser. Anal. 32, 378–395.

DeGaetano, A.T., Belcher, B.N., 2007. Spatial interpolation of daily maximum and minimum air temperature based on meteorological model analyses and independent observations. J. Appl. Meteorol. Climatol. 46, 1981–1992.

Donatelli, M., Magarey, R.D., Bregaglio, S., Willocquet, L., Whish, J.P.M., Savary, S., 2017. Modelling the impacts of pests and diseases on agricultural systems. Agric. Syst. 155, 213–224.

El Jarroudi, M., Delfosse, P., Maraite, H., Hoffmann, L., Tychon, B., 2009. Assessing the accuracy of simulation model for Septoria leaf blotch disease progress on winter wheat. Plant Dis. 93, 983–992.

El Jarroudi, M., Kouadio, L., Delfosse, P., Giraud, F., Junk, J., Hoffmann, L., Maraite, H., Tychon, B., 2012. Typology of the main fungal diseases affecting winter wheat in the Grand Duchy of Luxembourg. J. Agric. Sci. Technol. A 2, 1386–1399.

El Jarroudi, M., Kouadio, A.L., Mackels, C., Tychon, B., Delfosse, P., Bock, C.H., 2014. A comparison between visual estimates and image analysis measurements to determine Septoria leaf blotch severity in winter wheat. Plant Pathol. 64, 355–364.

El Jarroudi, M., Kouadio, L., Beyer, M., Junk, J., Hoffmann, L., Tychon, B., Maraite, H., Bock, C.H., Delfosse, P., 2015. Economics of a decision-support system for managing the main fungal diseases of winter wheat in the Grand-Duchy of Luxembourg. Field Crops Res. 172, 32–41.

Estrada-Pena, A., Estrada-Sanchez, A., de la Fuente, J., 2014. A global set of Fourier-transformed remotely sensed covariates for the description of abiotic niche in epidemiological studies of tick vector species. Parasites Vectors 7, 302.

Eyal, Z., 1999. The Septoria tritici and Stagonospora nodorum blotch diseases of wheat. Eur. J. Plant Pathol. 105, 629–641.

Filipe, J.A.N., Maule, M.M., 2004. Effects of dispersal mechanisms on spatio-temporal development of epidemics. J. Theor. Biol. 226, 125–141.

Fones, H., Gurr, S., 2015. The impact of Septoria tritici Blotch disease on wheat: an EU perspective. Fungal Genet. Biol. 79, 3–7.

Garrett, K.A., Forbes, G.A., Savary, S., Skelsey, P., Sparks, A.H., Valdivia, C., van Bruggen, A.H.C., Willocquet, L., Djurle, A., Duveiller, E., Eckersten, H., Pande, S., Vera Cruz, C., Yuen, J., 2011. Complexity in climate-change impacts: an analytical framework for effects mediated by plant disease. Plant Pathol. 60, 15–30.

Gilliam, R.C., Hogrefe, C., Rao, S.T., 2006. New methods for evaluating meteorological models used in air quality applications. Atmos. Environ. 40, 5073–5086.

Gladders, P., Paveley, N.D., Barrie, I.A., Hardwick, N.V., Hims, M.J., Langton, S., Taylor, M.C., 2001. Agronomic and meteorological factors affecting the severity of leaf blotch caused by Mycosphaerella graminicola in commercial wheat crops in England. Ann. Appl. Biol. 138, 301–311.

Hahn, F., 2002. AE—automation and emerging technologies: fungal spore detection on tomatoes using spectral Fourier signatures. Biosyst. Eng. 81, 249–259.

Hartkamp, A.D., De Beurs, K., Stein, A., White, J.W., 1999. Interpolation Techniques for Climate Variables. NRG-GIS Series 99-01. CIMMYT, Mexico, D.F p. 32.

Henshall, W.R., Hill, G.N., Beresford, R.M., Agnew, R.H., Wood, P.N., Marshall, R.R., 2016. Functional development of a New Zealand weather station network to improve plant production. N. Z. Plant Protect. 69, 120–125.

Hogrefe, C., Rao, S.T., Zurbenko, I.G., Porter, P.S., 2000. Interpreting the information in ozone observations and model predictions relevant to regulatory policies in the Eastern United States. Bull. Am. Meteorol. Soc. 81, 2083–2106.

Horne, J.H., Baliunas, S.L., 1986. A prescription for period analysis of unevenly sampled time series. Astrophys. J. 302, 757–763.

Jones, S.J., Gent, D.H., Pethybridge, S.J., Hay, F.S., 2012. Site-specific risk factors of white mould epidemics in bean (Phaseolus vulgaris) in Tasmania, Australia. N. Z. J. Crop Hort. Sci. 40, 147–159.

Jones, R.H., 1964. Spectral analysis and linear prediction of meteorological time series. J. Appl. Meteorol. 3, 45–52.

Junk, J., Görgen, K., El Jarroudi, M., Delfosse, P., Pfister, L., Hoffmann, L., 2008. Operational application and improvements of the disease risk forecast model PROCULTURE to optimize fungicides spray for the Septoria leaf blotch disease in winter wheat in Luxembourg. Adv. Sci. Res. 2, 57–60.

Junk, J., Jonas, M., Eickermann, M., 2016. Assessing meteorological key factors on crop invasion by pollen beetle (*Meligethes aeneus* F.)—past observations and future perspectives. Meteorol. Z. 25 (No. 4), 357–364.

Kuuseoks, E., Liechty, H.O., Reed, D.D., Dong, J., 1997. Relating site-specific weather data to regional monitoring networks in the Lake States. For. Sci. 43, 447–452.

Lam, N.S.-N., 1983. Spatial interpolation methods: a review. Am. Cartogr. 10, 129–150.

Langvad, A.M., Noe, E., 2006. (Re)-innovating tools for decision-support in the light of farmers' various strategies. In: Langeveld, H., Röling, N. (Eds.), Changing European Farming Systems for a Better Future–new Visions for Rural Areas. Wageningen, The Netherlands, pp. 335–339.

Lovell, D.J., Parker, S.R., Hunter, T., Royle, D.J., Coker, R.R., 1997. Influence of crop growth and structure on the risk of epidemics by *Mycosphaerella graminicola* (*Septoria tritici*) in winter wheat. Plant Pathol. 46, 126–138.

Lovell, D.J., Hunter, T., Powers, S.J., Parker, S.R., Van den Bosch, F., 2004. Effect of temperature on latent period of septoria leaf blotch on winter wheat under outdoor conditions. Plant Pathol. 53, 170–181.

Lucas, J.A., 2011. Advances in plant disease and pest management. J. Agric. Sci. 149, 91–114.

Magarey, R.D., Seem, R.C., Russo, J.M., Zack, J.W., Waight, K.T., Travis, J.W., Oudemans, P.V., 2001. Site-specific weather information without on-site sensors. Plant Dis. 85, 1216–1226.

Mahtour, A., El Jarroudi, M., Delobbe, L., Hoffmann, L., Maraite, H., Tychon, B., 2011. Site-specific Septoria leaf blotch risk assessment in winter wheat using weather-radar rainfall estimates. Plant Dis. 95, 384–393.

Mikosch, T., Zhao, Y., 2014. A Fourier analysis of extreme events. Bernoulli 803–845.

Moreau, J.M., Maraite, H., 1999. Integration of knowledge on wheat phenology and Septoria tritici epidemiology into a disease risk simulation model validated in Belgium. Asp. Appl. Biol. 55, 1–6.

Moreau, J.M., Maraite, H., 2000. Development of an interaction decision-support system on a web site for control of *Mycosphaerella graminicola* in winter wheat. Bull. OEPV/EPPO 30, 161–163.

R Development Core Team, 2014. R: A Language and Environment for Statistical Computing. R Foundation for Statistical Computing, Vienna, Austria. http://www.R-project.org/.

Shaw, M.W., Royle, D.J., 1993. Factors determining the severity of epidemics of *Mycosphaerella graminicola* (*Septoria tritici*) on winter wheat in the UK. Plant Pathol. 42, 882–899.

Shaw, M.W., 1994a. Modeling stochastic processes in plant pathology. Annu. Rev. Phytopathol. 32, 523–544.

Shaw, M.W., 1994b. Seasonally induced chaotic dynamics and their implications in models of plant disease. Plant Pathol. 43, 790–801.

Shtienberg, D., 2013. Will decision-support systems be widely used for the management of plant diseases? Annu. Rev. Phytopathol. 51, 1–16.

Small, I.M., Joseph, L., Fry, W.E., 2015. Development and implementation of the BlightPro decision support system for potato and tomato late blight management. Comput. Electron. Agric. 115, 57–65.

Suffert, F., Sache, I., Lannou, C., 2011. Early stages of septoria tritici blotch epidemics of winter wheat: build-up, overseasoning, and release of primary inoculum. Plant Pathol. 60, 166–177.

Te Beest, D., Shaw, M., Pietravalle, S., van den Bosch, F., 2009. A predictive model for early-warning of Septoria leaf blotch on winter wheat. Eur. J. Plant Pathol. 124, 413–425.

Verreet, J.A., Klink, H., Hoffmann, G.M., 2000. Regional monitoring for disease prediction and optimization of plant protection measures: the IPM wheat model. Plant Dis. 84, 816–826.

Zadoks, J.C., Chang, T.T., Konzak, C.F., 1974. A decimal code for the growth stages of cereals. Weed Res. 14, 415–421.

Zurbenko, I.G., 1986. The spectral analysis of time series. North-Holland, Amsterdam.